Comparison of solids suspension criteria based on electrical impedance tomography and visual measurements

Petri Tervasmäki*, Jari Tiihonen, Heikki Ojamo

*Corresponding author, petri.tervasmaki@oulu.fi, +358 40 5474973

Abstract

Different approaches have been adopted to quantify the performance of stirred vessels in suspending sinking solids into liquid phase. In this study we used electrical impedance tomography (EIT) to estimate the solids distribution in a lab-scale stirred vessel with a diameter of 362 mm. Also visual measurements were made to determine the cloud height and just suspended impeller speed. Quartz sand with a density of 2650 kg/m^3 was employed as the solid phase with different particle size fractions from 50 to 180 µm and solids volume fractions of 7.5 and 15 %. The effect of impeller type was studied by using two axial flow impellers, a pitched blade turbine and a hydrofoil impeller.

Two different states – partial and homogeneous suspension – were defined from the EIT data in addition to visual measurement of complete off-bottom suspension and cloud height. Partial suspension was determined from the EIT data, and it was reached at relatively low agitation rates. Visual measurements and data from the literature also support this observation, and EIT was proved to be a suitable method to quantify a repeatable partial suspension criterion. Complete off-bottom suspension was measured visually by determining the agitation rate at which there were no stationary solid particles at the vessel bottom for longer than 2 seconds. However, the applicability of this widely used criterion was questioned in the case of dense suspensions of small particles. Homogeneous suspension was estimated from the EIT data, and it was reached by approximately doubling the impeller revolution rate from the partial suspension criterion. The hydrofoil impeller reached all states of suspension with lower power consumption compared to the pitched blade turbine.

Keywords

Solid-liquid mixing; electrical impedance tomography; homogeneity; suspension criteria; axial flow impeller

1 Introduction

Solid-liquid suspensions are encountered frequently in different areas of process industries, and stirred vessels used in mixing the two phases have been under extensive research for decades. Factors that affect the suspension of solid particles to the liquid phase include physical properties of solid and liquid phases, the fraction of solids relative to liquid, geometric parameters of the system and agitation conditions. The state of suspension is often divided into three separate criteria, on-bottom motion (or partial suspension), off-bottom suspension and homogeneous suspension (Atiemo-Obeng et al., 2004). Partial suspension is defined as a state at which most of the solids are moving at the vessel bottom excluding a formation of fillets at some parts. Off-bottom suspension (or complete suspension or just suspended impeller speed, N_{js}) was first defined by Zwietering (1958) as an agitation rate at which no particles remain at the vessel bottom for more than 1 – 2 s. Homogeneous suspension refers to a state in which the particles are uniformly distributed throughout the vessel. The definition of partial suspension is rather broad and there are different approaches to experimentally measure this state of suspension (Bujalski et al., 1999;Chudacek, 1986;Micale et al., 2002). N_{js} and homogeneous suspension are clearly defined. However, the applicability of N_{js} is questionable for dense suspensions of small particles (Kraume and Zehner, 2001), and the determination of homogeneous suspension requires more detailed knowledge of the distribution of the solid phase.

Several methods have been used to assess the state of suspension. Visual methods are simple and can be used to determine the just suspended impeller speed (N_{js}) and a level at which the solids rise at a certain agitation rate, usually referred to as cloud height (CH). Micale et al. (2002) used a pressure gauge at the vessel bottom to determine the fraction of suspended solids in relation to total solids. Kraume (1992) and Bujalski et al. (1999) compared different visual states of suspension (cloud height, N_{js}) to mixing time and concluded that the effect of solids on the mixing time compared to the mixing time of liquid alone can be divided into the following phases. First, when only a small fraction is suspended, the mixing time of the suspension is similar to the case of liquid only. At this point, the liquid circulates efficiently and the few suspended particles may be distributed almost throughout the vessel. With increasing agitation, a larger fraction of the particles are suspended resulting in a non-steady circulating flow and decreased cloud height. The longest mixing time is measured at this point and a further increase in the agitation rate increases the cloud height while the mixing time decreases. These methods describe the state of suspension to some extent but they fail to give detailed information on the distribution of solids inside the vessel.

Local solids concentration can be measured either by direct sampling (Barresi and Baldi, 1987;MacTaggart et al., 1993) or indirectly by comparing differences in the solids concentration to optical (Angst and Kraume, 2006;Ayazi Shamlou and Koutsakos, 1989;Fajner et al., 1985;Magelli et al., 1990;Magelli et al., 1991;Montante et al., 2003) or electrical (Špidla et al., 2005) properties of the suspension. As pointed out by MacTaggart et al. (1993), it is difficult to gain a representative sample from a complex two-phase flow, and optical methods are usually restricted by the solids concentration. Electrical impedance tomography also makes use of conductivity differences between the phases and has only recently been used to quantify solid-liquid mixing (Harrison et al., 2012;Hosseini et al., 2010;Stevenson et al., 2010;Tahvildarian et al., 2011). Other recent measurement methods which have been used to measure the distribution of solids include magnetic resonance imaging (Stevenson et al., 2010) and particle tracking methods such as positron emission particle tracking (PEPT) (Guida et al., 2011).

In this article, we apply electrical impedance tomography to measure the solids suspension and distribution in a stirred vessel with moderate to dense solids concentration (X_V = 7.5 – 15 %) and small particle sizes (< 180 µm). The results from the EIT-measurements are also compared with traditional visual measurements of N_{js} and cloud height. In addition, criteria to determine the states of partial and homogeneous suspension from the EIT data are presented.

2 Materials and Methods

2.1 Experimental Setup

The experiments were conducted in a flat-bottomed stirred vessel with an inner diameter T = 362 mm equipped with four baffles with a width of 0.12T. Impeller type, particle size of solids,

solids loading and agitation rates were varied during the experiments. Two types of impellers were used, a four-bladed pitched blade turbine (4PBT) with a blade angle of 45˚ and a diameter D = 155 mm and an Outotec OKTOP3200® which is a three-bladed hydrofoil impeller with D = 145 mm. The impellers are presented in Figure 1. Both impellers were positioned with an off-bottom clearance C = 0.9D.

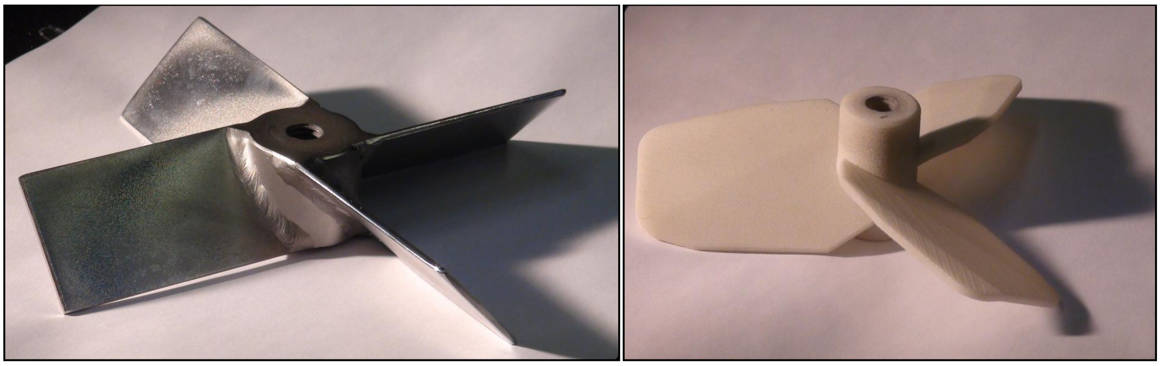

Figure 1. a) A 4-bladed pitched blade impeller with a blade angle of 45˚, D = 155 mm and b) OKTOP3200®, a 3-bladed hydrofoil impeller, D = 145 mm

Quartz sand with a density of 2650 kg/m^3 was sieved to known fractions of particle size, and the fractions that were used in the experiments were 50 – 75, 75 – 100 and 125 – 180 µm. Solids concentration varied from 200 to 400 g/l (volume fraction X_V = 7.5 – 15 %). Tap water at room temperature (22˚C) was used as the liquid phase. Each combination of impeller type and slurry properties (X_V and d_p) was measured at 13 agitation rates. Different ranges for impeller revolution rates were used depending on the impeller type and solids properties in order to reach all desired levels of suspension. Experimental conditions are presented in detail in Table 1.

Table 1. Solids concentration, particle size and agitation rates that were used for the experiments

X_V	d_p	N [rpm]	
%	µm	OKTOP3200®	4PBT
7.5	50-75	125 - 500	-
15	50-75	125 - 500	-
7.5	75-100	125 - 500	100 - 320
15	75-100	125 - 500	100 - 320
7.5	125-180	200 - 650	150 - 500
15	125-180	200 - 650	150 - 500

2.2 Electrical Impedance Tomography (EIT)

The stirred vessel was equipped with an electrical impedance tomography measurement system (Numcore Ltd, Finland). The Numcore EIT system consists of three operational blocks: the electrodes that form the interface between the process and the measurement system, an EIT-device that performs the current injection, voltage measurements and signal processing and, finally, a PC with software that generates the tomographic image. The details of the measurement system and image reconstruction are presented by Heikkinen et al. (2006).

Circular electrodes were attached to the inner surface of the vessel in nine planes with four electrodes per plane. A slightly modified opposite current injection strategy was used with a total of 28 independent current injections. An adjacent strategy, where voltages are measured from adjacent electrodes, was used for the voltage measurements. The solution domain based on the reactor geometry was discretized into a mesh consisting of tetrahedral elements with a total of 16032 elements and 76145 nodes. Reference data for the EIT-measurement were recorded from a vessel that was filled with water only. Baffles and other interiors were present during the reference data capture, and separate reference data sets were recorded for different impellers. Solids concentration at a certain conductivity value was calculated by the Equation (2.1).

$$X_{i,ms/Vtot} = \frac{\sigma_{max} - \sigma_i}{\sigma_{max} - \sigma_{avg}} \overline{X} \qquad \textbf{(2.1)}$$

Where $X_{i,ms/Vtot}$ is the solids concentration at height i [g_{solids} / l]

σ_{max} is the maximum conductivity of the vertical profile [mS/cm]

σ_{avg} is the average conductivity of the vertical profile [mS/cm]

σ_i is the conductivity at height i [mS/cm]

$\overline{X}$ is the average solids concentration [g_{solids} / l]

2.3 Other measurements

In addition to EIT, the suspension was also examined visually during the measurements. Cloud height was determined for each measurement as the height at which the solids remained stationary for some time. There were local bursts towards higher and lower cloud height, but a height at which the cloud height remained constant for some time could be distinguished. Also N_{js} was determined visually for each reactor and slurry configuration by observing the transparent bottom of the vessel in well-lit conditions so that movement of the particles could be distinguished. A criterion where no particles remained stationary for more than 2 seconds was used for N_{js}.

In order to measure power consumption, the vessel was placed on a table that rotates freely, and the force exerted by this rotation was measured with a force transducer. When, in addition to the measured force, the distance from the centre of the tank to the force transducer and impeller rotational speed are known, impeller power draw can be calculated by the Equation (2.2).

$$P = Fr2\pi N \quad \textbf{(2.2)}$$

where P is the power draw of the impeller [W]

F is the measured force [N]

r is the length of lever arm [m]

N is the impeller rotational speed [s^{-1}]

3 Results and Discussion

3.1 Suspension criterion from the EIT data

A typical EIT data set from one measurement is presented in Figure 2 where the average conductivity at three separate planes is plotted against time. Impeller revolution rate was increased stepwise from 125 to 500 rpm during the measurement. At the agitation rates from 125 to 190 rpm, some stationary solids were gradually lifted to the suspension and also sudden, occasional bursts of solids could be distinguished. These can be seen as a fluctuation of the conductivities during a constant agitation rate. At 210 rpm, however, the conductivity at the lowest plane reaches a minimum and a steady state of conductivity is reached throughout the vessel. Further increase in the agitation rate results in an almost instantaneous step change of the conductivities towards a more homogeneous suspension.

It can be concluded from the visual inspections that this condition of minimum conductivity at the bottom was not equal to the just suspended criterion N_{js} as suggested by Ayazi Shamlou and Koutsakos (1989) and Nienow (1997), but there were always stationary solid particles remaining at the vessel bottom. A similar trend was found for all measurements, and this state of suspension will be referred to as partial suspension criterion (N_{ps}) and can be interpreted as the maximum concentration of solids at the bottom part of the vessel. A further increase in the agitation rate still withdraws some stationary solids from the bottom but it also lifts more of the suspended solids to the upper parts of the vessel resulting in a decrease in the local solids concentration at the lower parts.

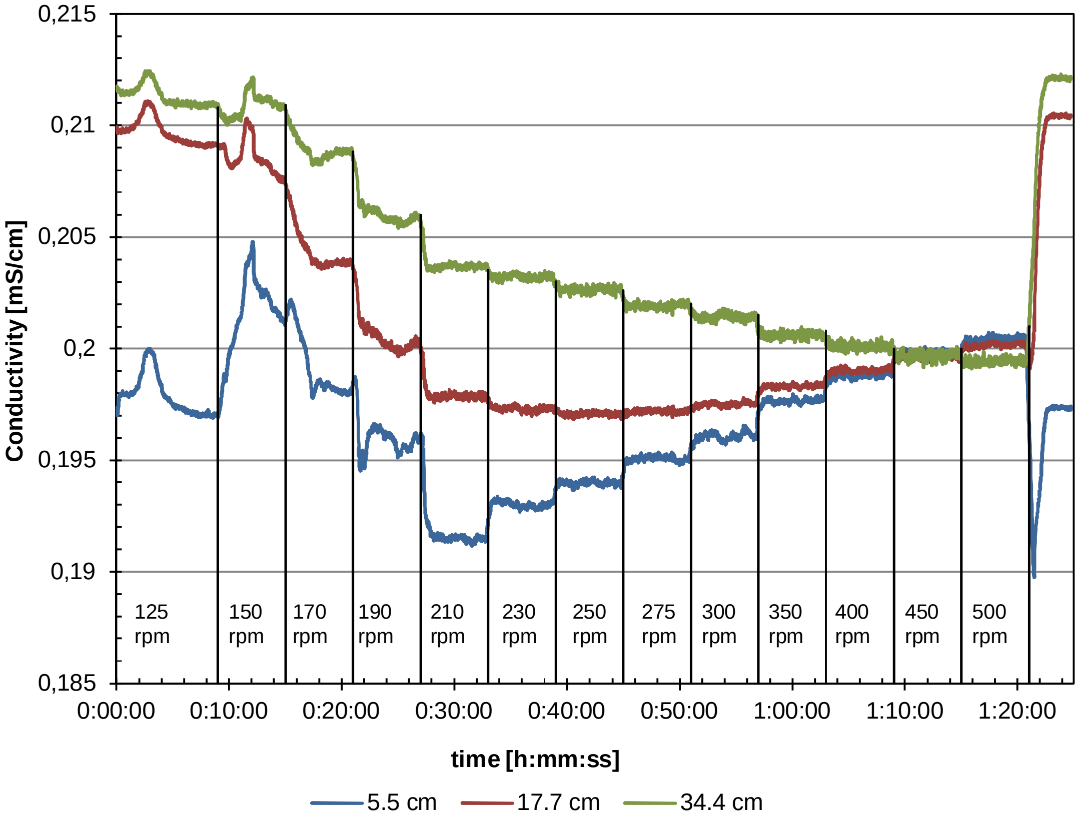

Figure 2. Conductivity at levels 5.5 cm (0.15 H), 17.7 cm (0.49 H) and 34.4 cm (0.95 H). OKTOP3200® impeller, 4 baffles, d_p = 75 – 100 µm, X_V = 7.5 %

A repetitive pattern was also found in cloud height measurements at N_{ps}. Below this agitation rate, cloud height either could not be determined, remained constant or even decreased with increasing agitation. Only above this agitation rate cloud height increased monotonically with agitation. This finding is similar to the one reported by Bujalski et al. (1999), Kraume (1992) and Michelett et al. (2003). For relevant particle sizes, the maximum mixing time occurs at agitation rates below N_{js} together with a discontinuity in cloud height. After reaching the maximum value, mixing time quickly decreases and cloud height increases with increased agitation. Micale et al. (2002) used a pressure gauge at the vessel bottom to assess the amount of unsuspended solids and fitted the data with a two-parameter model to calculate an impeller revolution rate at which 98 % of the particles were suspended. On average, an increase of 30 % in agitation rate was required to suspend the last 2 % of the particles resulting in a twofold increase in power consumption. Thus, 98 % suspension was referred as sufficient suspension,

N_{ss}. The relationship between N_{ps} and N_{js} in our experiments was somewhat similar, N_{js} being on average 40 % larger than N_{ps}. However, no clear correlation between the two suspension criteria could be established and the variation of N_{js} with respect to N_{ps} was quite high as will be pointed out in the next sections.

As a conclusion, it can be stated that the fluctuation in the EIT data at the low agitation rates can be explained by the non-steady circulating flow suggested by Kraume (1992) and the lowest applicable impeller revolution rate should always be above the partial suspension criterion. It is easy to determine from the EIT data and it gives more consistent results compared to the visual measurement of N_{js} which is problematic to determine especially for high solids concentrations and small particle sizes. The effect of geometric parameters and suspension properties on the partial suspension (N_{ps}) and N_{js} is assessed in later sections.

3.2 Homogeneous suspension

Beyond the partial suspension criterion, the homogeneity of the suspension can be assessed by calculating the relative standard deviation (RSD) of the axial concentration profile

$$RSD = \frac{1}{\bar{\bar{X}}}\sqrt{\frac{1}{n-1}\sum_{i=1}^{n}(X_i - \bar{X})^2} \quad \textbf{(3.1)}$$

where $\bar{X}$ is the mean solids fraction

X_i is the average solids fraction at measurement height i

n is the number of vertical data points

RSD of the axial concentration profile has been used by several authors (Hosseini et al., 2010;Jafari et al., 2012;Magelli et al., 1991;Tahvildarian et al., 2011;West et al., 1999) to quantify the effect of reactor geometry, suspension properties and impeller revolution rate on the homogeneity of solid-liquid suspension. RSD is plotted against power consumption for one reactor geometry with different slurry properties in Figure 3. It can be seen that the power required to reach a certain value of RSD is increased with increase in solids concentration and particle size. Also a point of minimum RSD, beyond which the value of RSD increases with increase in agitation power, can be distinguished. Similar findings have been reported in the literature (Harrison et al., 2012;Hosseini et al., 2010). However, the minimum value of RSD that was reached approached zero, independent of impeller type and slurry properties. This is in contrast with the results of Hosseini et al. (2010) who reported that a more homogeneous suspension can be attained depending on the impeller or the particle size and volume fraction of solids.

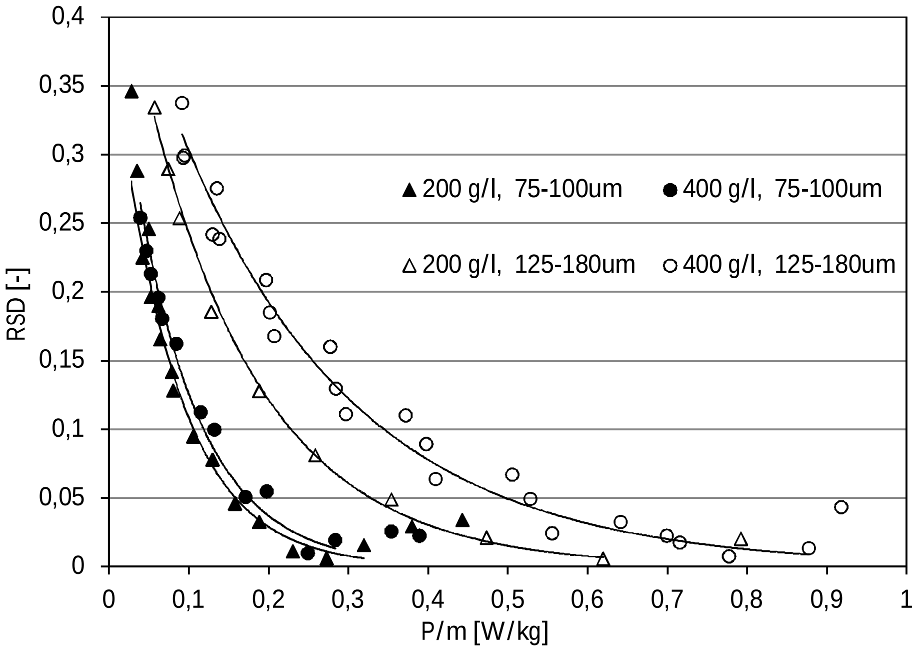

Figure 3 RSD vs. power consumption per unit mass for different slurries agitated with OKTOP3200® impeller. Exponential fit is provided for eye-guidance and is calculated only until the minimum value of RSD.

Distribution of the solid phase can also be assessed by one-dimensional sedimentation-dispersion model for a batch system in steady-state using Peclet-number (Pe) as an adjustable parameter (Montante et al., 2003):

$$\frac{X_V\left(\frac{z}{H}\right)}{\overline{X_V}} = \frac{Pe}{1-\exp(-Pe)}\exp\left(-Pe\frac{z}{H}\right) \quad \textbf{(3.2)}$$

$$Pe = \frac{U_s H}{D_{e,p}} \quad \textbf{(3.3)}$$

where z is the axial position [m]

$\overline{X_V}$ is the mean solids volume fraction

X_V is the solids volume fraction

H is the height of the liquid batch [m]

U_s is the settling velocity of solid particles in stirred medium [m/s]

$D_{e,p}$ is the dispersion coefficient for the solid phase [m^2/s]

Pe is the Peclet number (dimensionless adjustable parameter)

Steady-state can be assumed for $N \geq N_{ps}$ as verified by the EIT data and Pe was calculated from the experimental data for these agitation rates. Pe and RSD can be related analytically, and experimental values have been shown to correlate almost linearly by (Magelli et al., 1991). A linear relationship between Pe and RSD was established from our data as shown in Figure 4. The value of Pe decreases as homogeneity of the suspension increases but, unlike RSD, it does not have a minimum value at homogeneous suspension. Instead, it approaches zero as homogeneity increases and may yield negative values if solids concentration is higher at the top part of the vessel. Measured and fitted profiles for three impeller revolution rates are presented in Figure 5 where it can be seen that fitted Pe-number yields a negative value at 500 rpm and homogeneous suspension was reached with lower N. Thus, the most homogeneous suspension can be estimated to be between the agitation rates at which the value of Pe changes from positive to negative. Values for agitation rate (N_h), power consumption (P_h) and cloud height (CH_h) at Pe = 0 as presented later in the text were calculated by linear interpolation. The assumption of linearity is justified as the agitation rate was increased with intervals of 50 rpm or less. It should be noted that sedimentation-dispersion model gives, by definition, monotonical vertical profiles and cannot accommodate local inhomogeneties as shown in Figure 5.

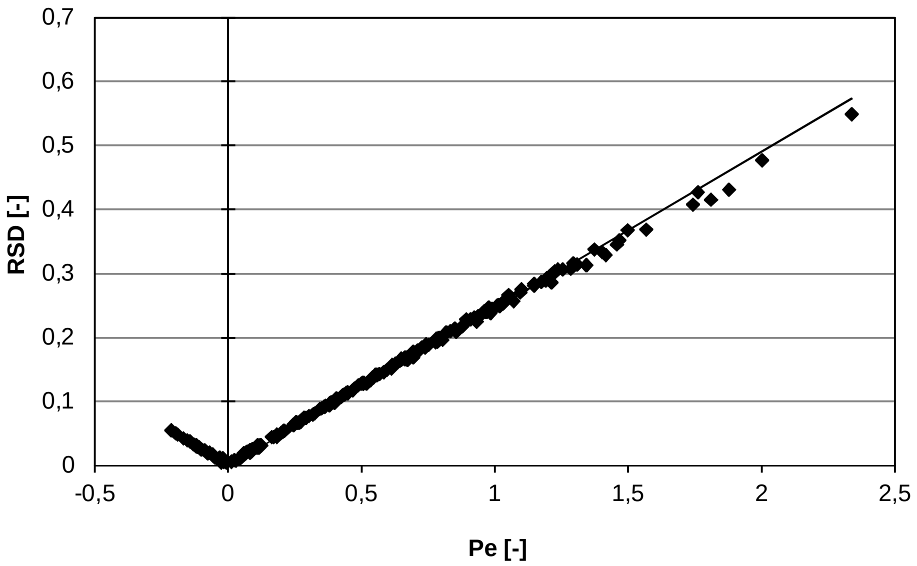

Figure 4 RSD vs. Pe for all measurements, RSD = 0.245Pe for Pe > 0

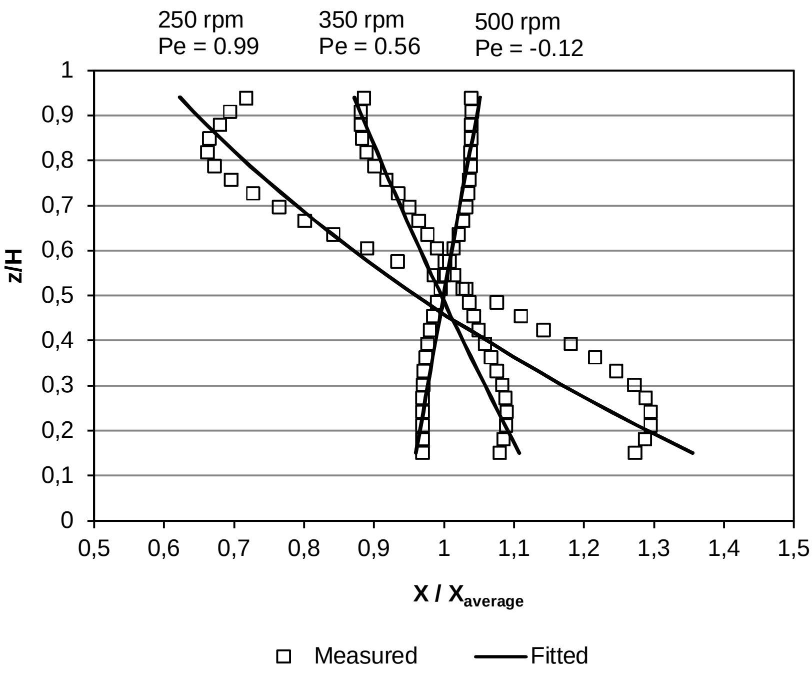

Figure 5 Dimensionless axial solid concentration profile and profile fitted with the equation (3.2). OKTOP3200® impeller, 4 baffles, d_p = 75 – 100 µm, X_V = 7.5 %

3.3 Comparison of Suspension Criteria

Three different suspension criteria – visually determined N_{js} as well as partial and homogeneous suspension from EIT data – were used in this study. For comparison, the values of N for each criterion are plotted against particle size for both impeller types and solids concentrations in Figure 6. Regression curves for power law equation $\left(N = a * d_p^b\right)$ are provided for eye-guidance.

Three particle size fractions were used in the measurements with OKTOP3200® hydrofoil impeller (Figure 6a). N_{ps} increases with particle size and for the range used in this work, N_{ps} can be related to d_p with an exponent of 0.41 ($N_{ps} \propto d_p^{0.41}$) The same is not true for N_{js}, which increases significantly from 50 – 75 to 75 – 100 µm but only slightly from 75 – 100 to 125 – 180 µm size fractions. Also the difference between N_{ps} and N_{js} decreases with increasing particle size. The values of N_h are significantly higher than N_{js} or N_{ps} for all particle sizes but the effect of particle size is similar as for partial suspension ($N_h \propto d_p^{0.41}$). Similar power law dependencies of N vs. particle size have been reported in the literature (Chudacek, 1986). However, the results presented here considering the power law dependence should be read with caution as only three fractions in a relatively narrow size range were tested and particle size distribution within the fractions is not known.

The measurements with the 4PBT were made with two particle size fractions (Figure 6b). The results follow similar trends as for OKTOP3200® but the N_{js} is closer to N_h rather than N_{ps}. Actually, for solids volume fraction of 47 % and particle size of 75 – 100 µm, N_{js} is higher than N_h. This further questions the applicability of just suspended criterion as the suspension of the last few particles depend highly on the specific flow pattern at the vessel bottom. The effect of solids concentration is similar for all suspension criteria and both impellers and it increases the required agitation rate.

Impeller revolution rates at N_h and N_{js} are plotted against N_{ps} for each measurement in Figure 7**.** It is interesting to note that there is a good linear correlation between agitation rates required for partial and homogeneous suspensions, the relationship being $N_h = 2N_{ps}$, independent of the stirrer type. N_{js} is always higher than the stirrer speed for partial suspension but no clear correlation is found between N_{js} and N_{ps}. The twofold increase in the agitation rate when moving from partial to homogeneous suspension results in a theoretical increase of power consumption by a factor of 8. The largest values of power consumption are encountered for the largest particle size fraction for which the volumetric power consumption is around 1000 W/m^3 at the homogeneous suspension for both impellers. It should be noted that typically the volumetric power consumption decreases in scale-up from laboratory to industrial scale depending on the suspension criterion and system geometry (Chudacek, 1986;Montante et al., 2003). Thus the volumetric power consumption of 1000 W/m^3 for homogeneous suspension in the laboratory scale does not unambiguously mean similar power consumption in the large scale industrial processes. However, the discussion of scale-up is out of the scope of this paper and is not continued here. Significant increase in the power consumption when moving from N_{ps} to N_{js} and N_h still suggests that the sufficient state of suspension should be optimized between partial and homogeneous suspension. The sufficient state is process specific and may be related to reaction kinetics in leaching or crystallization reactors or simply a task of providing a homogeneous material outflow from a continuous mixing tank.

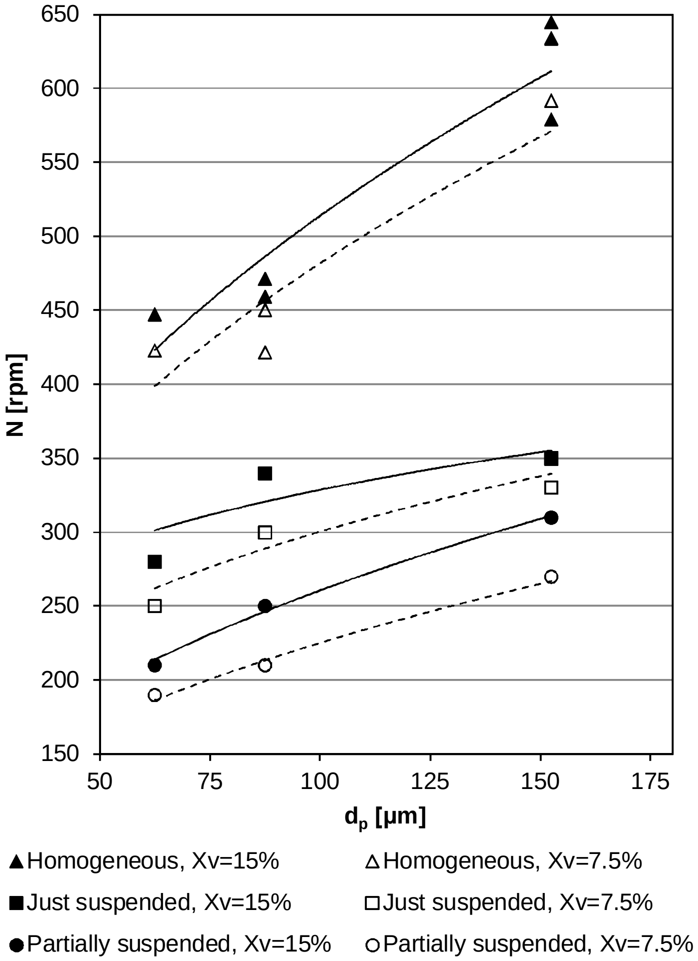
N [rpm]
650
600
550
500
450
400
350
300
250
200
150
50
75
100
125
150
175
d_p [μm]
Homogeneous, Xv=15%
Homogeneous, Xv=7.5%
Just suspended, Xv=15%
Just suspended, Xv=7.5%
Partially suspended, Xv=15%
Partially suspended, Xv=7.5%

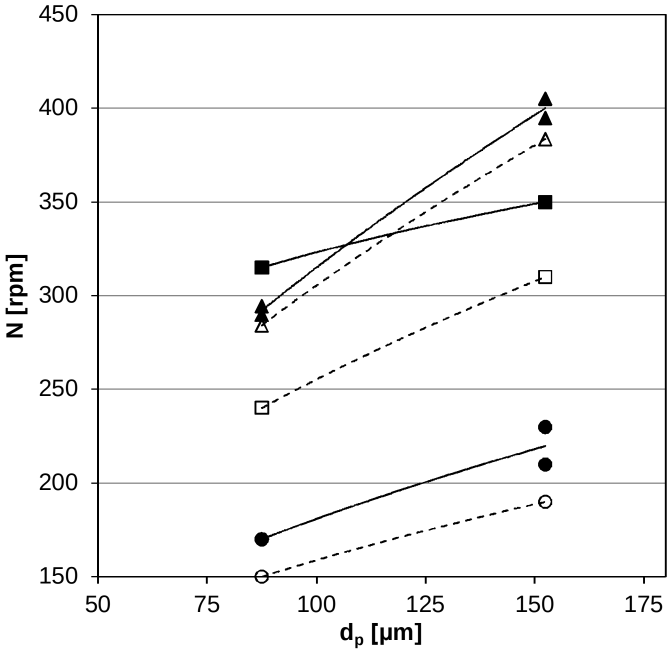
N [rpm]
450
400
350
300
250
200
150
50
75
100
125
150
175
d_p [μm]

Figure 6 Agitation rate vs. particle size for different suspension criteria and impellers. The arithmetic mean of the limiting particle sizes of each fraction is used as d_p. a) OKTOP3200® b) 4BPT

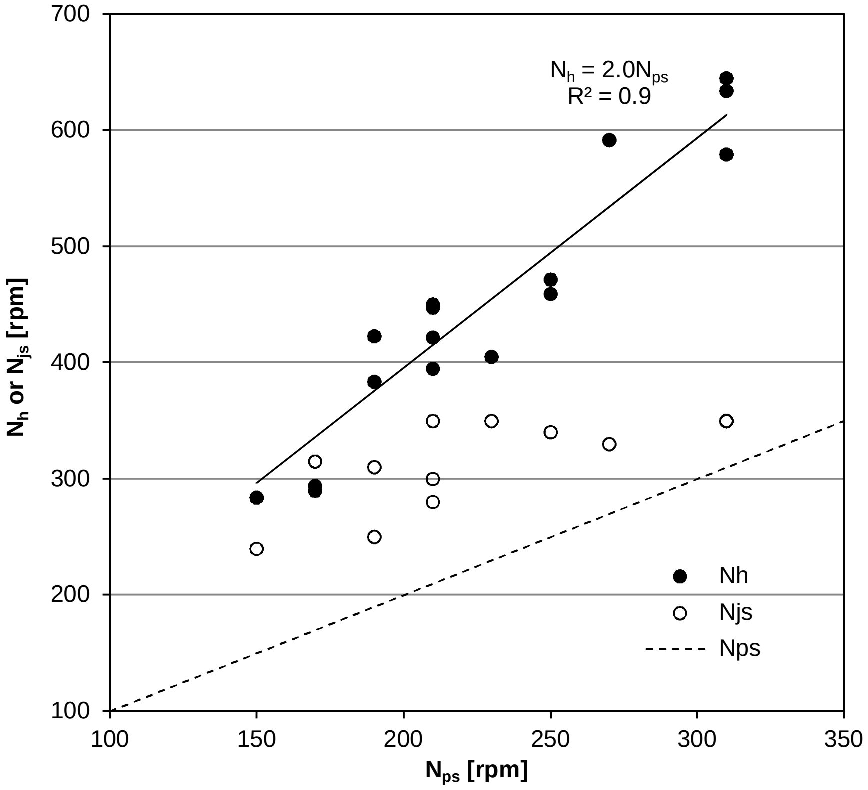

Figure 7 N_h and N_{js} vs. N_{ps} for all measurements

Two impeller types are compared in terms of power consumption in Figure 8 where the power per unit mass required for partial and homogeneous suspensions is plotted for both the impeller types and different slurry properties. This figure further illustrates the substantial increase in power consumption when moving from partial to homogeneous suspension. The power consumption of the hydrofoil impeller is less than the power consumption of the pitched blade impeller for all suspension states and slurry properties. Similar results have been reported by other authors (Hosseini et al., 2010;Tahvildarian et al., 2011). For the partial suspension criterion, the difference between the impellers is rather large as the hydrofoil impeller consumes only 56 – 72 % of the power required by the pitched blade impeller, depending on the particle size and solids fraction. Similar figures for homogeneous suspension fall between 73 – 94 %. Increase in the concentration of solids (X_V) from 7.5 to 15 % makes the two impellers more even and the smallest difference between the impellers is at the higher solids concentration.

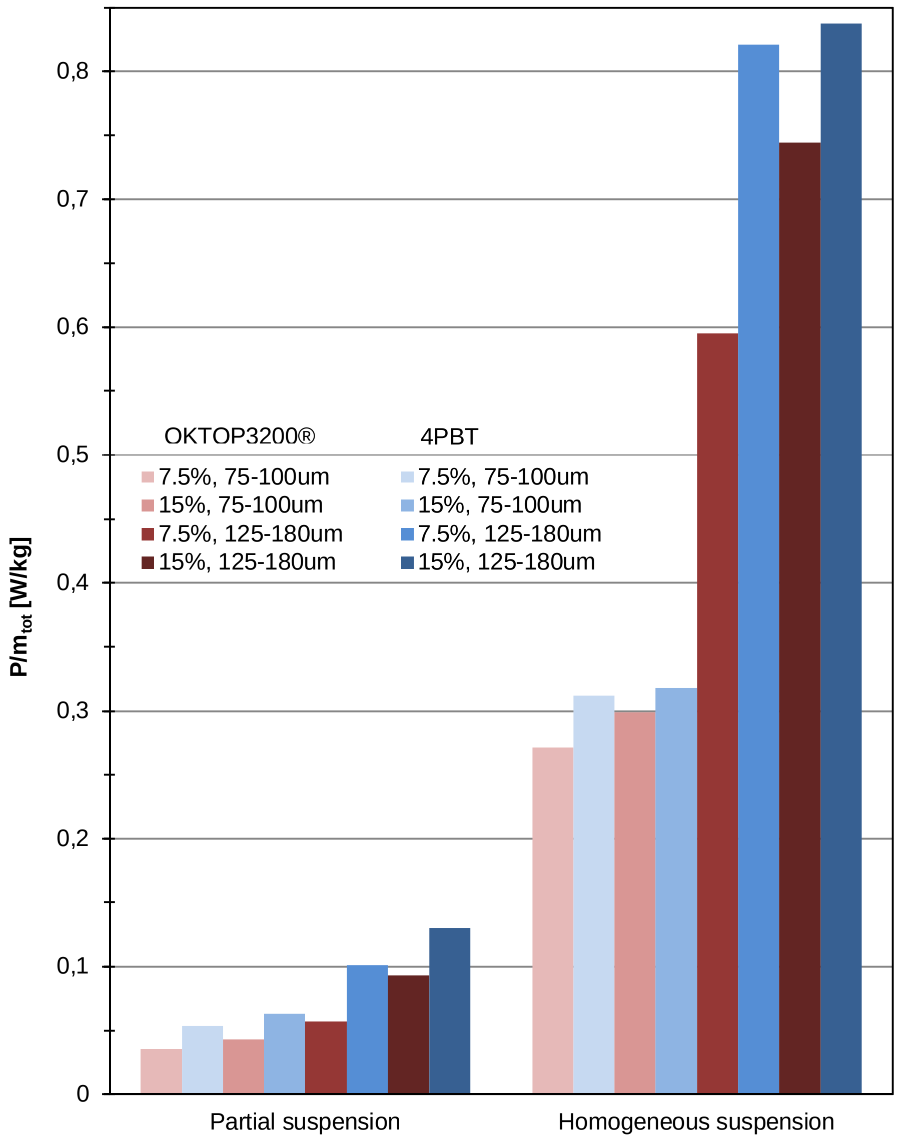

Figure 8 Power consumption per total mass of slurry at N_{ps} and N_h.

As noted previously, behaviour of cloud height was different for agitation rates below and above N_{ps}. This is illustrated in Figure 9 where dimensionless cloud height is plotted against N for two measurements and, clearly, the cloud height starts to increase monotonically only after N_{ps}. Homogeneous suspension was reached at cloud heights > 0.9. A histogram of cloud height that was reached at partial and homogeneous suspension is plotted in Figure 10. Cloud height at N_{ps} is more scattered between 0.63 and 0.77 with an average of 0.69 whereas cloud height at N_h is more sharply concentrated between 0.92 and 0.98 with an average of 0.96. This is quite close to the value of 0.95, which has been used by (Chudacek, 1986) to determine a homogeneous suspension. The scattering of cloud height at N_{ps} can be expected as the partial suspension criterion is based only on the changes of solid concentration at the lower parts of the vessel. Total solids concentration has an effect on cloud height at N_{ps} as can be seen from Figure 10. With less solids to be suspended (X_V = 7.5 %), N_{ps} is reached with lower agitation rates, and cloud height remains lower when compared to higher solids concentration (X_V = 15 %). In order to reach homogeneous suspension, however, solids have to be distributed throughout the vessel, and the cloud height has to be sufficient for this suspension criterion.

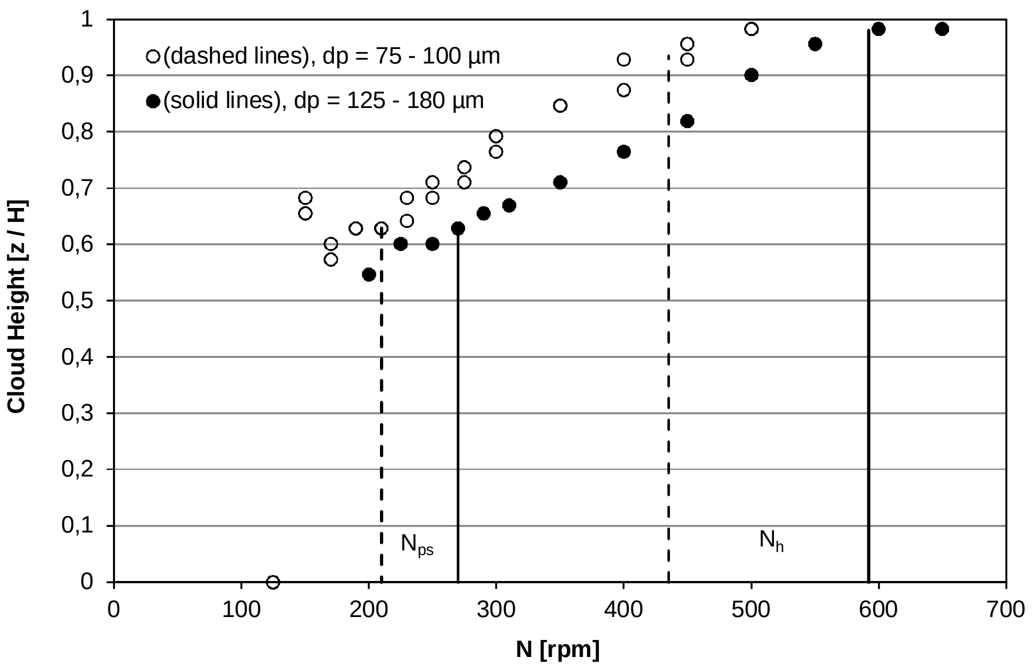

Figure 9 Dimensionless cloud height vs. impeller revolution rate for two different particle size fractions agitated with OKTOP3200® impeller, X_V = 7,5 %.

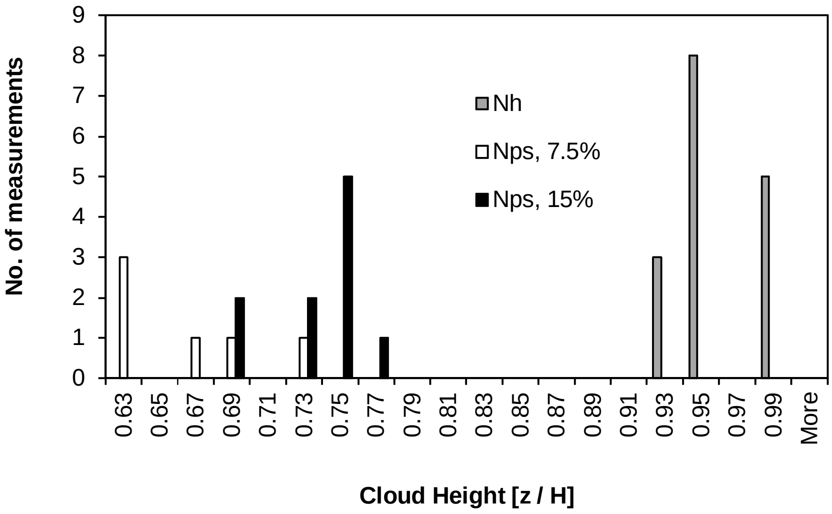

Figure 10 Histogram of cloud height at N_{ps} and N_{js} for all measurements

4 Conclusions

Suspension of solid particles in liquid was measured by electrical impedance tomography (EIT) and visual inspection. EIT data were used to determine two different suspension criteria, partial and homogeneous suspension. Partial suspension was defined to be the agitation rate at which the solids concentration at the lowest plane of electrodes reaches a maximum. It was also shown that this is the lowest agitation rate at which the average axial solids distribution, measured by EIT, reaches a steady state. It was also found from the visual measurements that cloud height began to increase monotonically with agitation only at agitation rates above N_{ps}. Similar suspension criterion has previously been described by several authors. A significant increase in the agitation rate and power was still required in order to suspend the rest of the particles and reach the complete suspension criterion (N_{js}). There was no clear correlation between N_{ps} and N_{js} which further questions the applicability of the complete suspension criterion to suspension of small particles and high solids concentrations.

Even further increase in the impeller revolution rate was required to reach homogeneous suspension, which was determined from the EIT data, and a good correlation between N_{ps} and N_h was established. Dimensionless cloud height at N_h was found to be almost equal to 0.95 which has previously been used to describe a homogeneous suspension. Outotec OKTOP3200® hydrofoil impeller reached all of the used suspension criteria with less power consumption compared to the 4-bladed pitched blade turbine. Electrical impedance tomography was proved to be applicable to determine the level of suspension in a wide range of suspension criteria. Therefore, EIT can be used to optimize – not only the geometry of the vessel and impeller – but also the state of suspension for a specific process.

Nomenclature

C	is impeller off-bottom clearance [m]
CH	is cloud height [m] or [-]
D	is impeller diameter [m]
$D_{e,p}$	is the dispersion coefficient for the solid phase [m^2/s]
d_p	is particle diameter [m]
H	is liquid height [m]
m	is mass [kg]
N	is impeller revolution rate [s^{-1}]
P	is power [W]
T	is tank diameter [m]
U_s	is the settling velocity of solid particles in stirred medium [m/s]
V	is suspension volume [m^3]
X	is the solids concentration (see subscripts for details)
z	is axial position [m]

Greek letters

σ	is conductivity [mS/cm]

Subscripts

js	complete suspension
ps	partial suspension
h	homogeneous suspension
ms/Vtot	mass of solids per total volume [g / l]
ms/ml	mass of solids per mass of liquid [kg_{solids} / kg_{liquid}]
V	solids volume fraction [m^3_{solids} / m^3_{tot}]

References

Angst, R., Kraume, M., 2006. Experimental investigations of stirred solid/liquid systems in three different scales: Particle distribution and power consumption, Chemical Engineering Science 61(9), 2864-2870.

Atiemo-Obeng, V. A., Penney, W. R., Armenante, P., 2004. Solid-Liquid Mixing, in: Handbook of Industrial Mixing, John Wiley & Sons, Inc., pp. 543-584.

Ayazi Shamlou, P., Koutsakos, E., 1989. Solids suspension and distribution in liquids under turbulent agitation, Chemical Engineering Science 44(3), 529-542.

Barresi, A., Baldi, G., 1987. Solid dispersion in an agitated vessel, Chemical Engineering Science 42(12), 2949-2956.

Bujalski, W., Takenaka, K., Paolini, S., Jahoda, M., Paglianti, A., Takahashi, K., Nienow, A. W., Etchells, A. W., 1999. Suspension and liquid homogenization in high solids concentration stirred chemical reactors, Chemical Engineering Research and Design 77(3), 241-247.

Chudacek, M. W., 1986. Relationships between solids suspension criteria, mechanism of suspension, tank geometry, and scale-up parameters in stirred tanks, Industrial and Engineering Chemistry Fundamentals 25(3), 391-401.

Fajner, D., Magelli, F., Nocentini, M., Pasquali, G., 1985. SOLIDS CONCENTRATION PROFILES IN A MECHANICALLY STIRRED AND STAGED COLUMN SLURRY REACTOR. Chemical Engineering Research and Design 63(4), 235-240.

Guida, A., Nienow, A. W., Barigou, M., 2011. Mixing of dense binary suspensions: Multi-component hydrodynamics and spatial phase distribution by PEPT, AIChE Journal 57(9), 2302-2315.

Harrison, S. T. L., Stevenson, R., Cilliers, J. J., 2012. Assessing solids concentration homogeneity in Rushton-agitated slurry reactors using electrical resistance tomography (ERT), Chemical Engineering Science 71, 392-399.

Heikkinen, L. M., Kourunen, J., Savolainen, T., Vauhkonen, P. J., Kaipio, J. P., Vauhkonen, M., 2006. Real time three-dimensional electrical impedance tomography applied in multiphase flow imaging, Measurement Science and Technology 17(8), 2083-2087.

Hosseini, S., Patel, D., Ein-Mozaffari, F., Mehrvar, M., 2010. Study of solid–liquid mixing in agitated tanks through electrical resistance tomography, Chemical Engineering Science 65(4), 1374-1384.

Jafari, R., Tanguy, P. A., Chaouki, J., 2012. Experimental investigation on solid dispersion, power consumption and scale-up in moderate to dense solid–liquid suspensions, Chemical Engineering Research and Design 90(2), 201-212.

Kraume, M., Zehner, P., 2001. Experience with experimental standards for measurements of various parameters in stirred tanks: A comparative test, Chemical Engineering Research and Design 79(8), 811-818.

Kraume, M., 1992. Mixing times in stirred suspensions, Chemical Engineering and Technology 15(5), 313-318.

MacTaggart, R. S., Nasr-El-Din, H. A., Masliyah, J. H., 1993. Sample withdrawal from a slurry mixing tank, Chemical Engineering Science 48(5), 921-931.

Magelli, F., Fajner, D., Nocentini, M., Pasquali, G., 1990. Solid distribution in vessels stirred with multiple impellers, Chemical Engineering Science 45(3), 615-625.

Magelli, F., Fajner, D., Nocentini, M., Pasquali, G., Marisko, V., Ditl, P., 1991. Solids concentration distribution in slurry reactors stirred with multiple axial impellers, Chemical Engineering and Processing 29(1), 27-32.

Micale, G., Grisafi, F., Brucato, A., 2002. Assessment of Particle Suspension Conditions in Stirred Vessels by Means of Pressure Gauge Technique, Chemical Engineering Research and Design 80(8), 893-902.

Michelett, M., Nikiforaki, L., Lee, K. C., Yianneskis, M., 2003. Particle Concentration and Mixing Characteristics of Moderate-to-Dense Solid-Liquid Suspensions, Industrial and Engineering Chemistry Research 42(24), 6236-6249.

Montante, G., Pinelli, D., Magelli, F., 2003. Scale-up criteria for the solids distribution in slurry reactors stirred with multiple impellers, Chemical Engineering Science 58(23–24), 5363-5372.

Nienow, A. W., 1997. Chapter 16 - The suspension of solid particles, in: N Harnby A2M.F. Edwards and A.W. NienowA2 N Harnby,M.F.Edwards, A.W. Nienow (Eds), Mixing in the Process Industries. Oxford, Butterworth-Heinemann, pp. 364-393.

Špidla, M., Sinevič, V., Jahoda, M., MacHoň, V., 2005. Solid particle distribution of moderately concentrated suspensions in a pilot plant stirred vessel, Chemical Engineering Journal 113(1), 73-82.

Stevenson, R., Harrison, S. T. L., Mantle, M. D., Sederman, A. J., Moraczewski, T. L., Johns, M. L., 2010. Analysis of partial suspension in stirred mixing cells using both MRI and ERT, Chemical Engineering Science 65(4), 1385-1393.

Tahvildarian, P., Ng, H., D'Amato, M., Drappel, S., Ein-Mozaffari, F., Upreti, S. R., 2011. Using electrical resistance tomography images to characterize the mixing of micron-sized polymeric particles in a slurry reactor, Chemical Engineering Journal 172(1), 517-525.

West, R. M., Jia, X., Williams, R. A., 1999. Quantification of solid-liquid mixing using electrical resistance and positron emission tomography, Chemical Engineering Communications 175, 71-97.

Zwietering, T. N., 1958. Suspending of solid particles in liquid by agitators, Chemical Engineering Science 8(3-4), 244-253.